On the possibility of magnetic flux detection by Andreev quantum dot

I. A. Sadovskyy[*1)], G. B. Lesovik[*], G. Blatter[▽]

[*] L. D. Landau Institute for Theoretical Physics RAS, 117940 Moscow, Russia

[▽] Theoretische Physik, ETH-Zurich, CH-8093 Zürich, Switzerland

Submitted 19 June 2007

The charge of subgap state in Andreev quantum dot (AQD) inserted into the superconducting loop is very sensitive to the magnetic flux threading the loop. We studied the sensitivity as a function of AQD parameters in details in $\Delta \to \infty$ limit. We also accounted for a weak Coulomb interaction in AQD. We discuss a possibility of using this setup as a device detecting week magnetic field.

PACS: 73.21.La, 74.45.+c, 07.55.Ge

1. Introduction. Josephson effect [1] has been intensively studying last 45 years. In this effect between two bulk superconductors separated by normal material appear a non-dissipative current, which depends on the superconducting phase difference φ. Recently a new development concerning Josephson junctions has appeared: a charge of normal part between two superconductors also depends on superconducting phase difference [2, 3]. This dependence is strong enough [2] and one may think about using this effect in a magnetic flux measuring device, although our estimation gives sensitivity somewhat below the sensitivity of the best by superconducting quantum interference devices (SQUIDs) (see below for more detailed discussions).

Usually small magnetic fields are measured SQUIDs [4, 5]. While SQUIDs are based on Josephson current dependence on superconducting phase difference φ (and hence on the magnetic flux Φ), we propose to use Andreev quantum dot charge dependence on φ. Andreev quantum dot (AQD) is a quantum dot inserted between superconducting banks with the superconducting gap Δ. As shown in [2], the charge Q of single-channel AQD can be fractional $-|e| < Q < |e|$ and depends on φ. Here $e = -|e|$ is the charge of one electron.

The charge of AQD can be measured by a sensitive charge detector, e.g. single-electron transistor (SET). The best SETs have sensitivity of the order $10^{-5} |e|/\sqrt{Hz}$ (e.g. see [6]). Using results of [2] one can make simple estimations and obtain that AQD can convert change of the flux $\delta\Phi$ to the change in charge δQ with the ratio $\delta Q/\delta\Phi = 2|e|/\Phi_0$, where $\Phi_0 = 2\pi\hbar/2|e|$ is the superconducting flux. Assuming that superconducting loop area is about $1\,\mathrm{mm}^2$, we obtain the sensitivity $10^{-14}\,T/\sqrt{Hz}$ which is comparable with the best

SQUIDs sensitivity $10^{-14} \div 10^{-15}\,T/\sqrt{Hz}$ [4, 5]. Below we study in details the ratio $\delta Q/\delta\Phi$ (which we called sensitivity).

2. Setup. The main part of the setup is Andreev quantum dot inserted into superconducting loop (Fig.1). AQD is supposed to be quasi-one dimensional normal
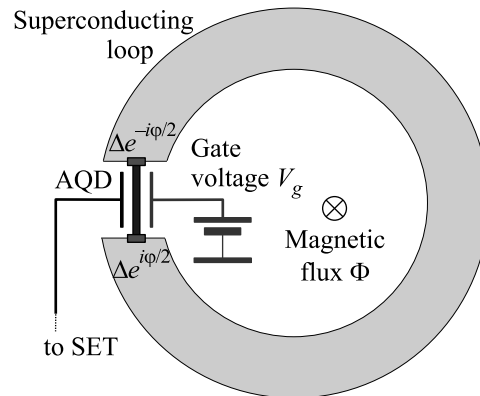

Fig.1. Andreev quantum dot inserted into the superconducting loop. AQD is connected to the single electron transistor (SET) and gate electrode through capacitive coupling. The flux Φ produces phase difference $\varphi = 2\pi\Phi/\Phi_0$ at AQD. The charge of AQD can be tuned by V_g and Φ

metal (N) separated from superconductors (S) by a normal scatterers (I). The position of the normal resonance in this SINIS system can be tuned by the gate voltage V_g applied to the normal region of AQD. The magnetic flux threading the loop Φ induces superconducting phase drop at AQD φ. Since the phase drop in the bulk superconductor is negligible comparing to the phase drop at AQD one may put $\varphi = 2\pi\Phi/\Phi_0$.

The single-electron transistor is connected to the normal region of AQD through capacitive coupling.

Experimentally such AQDs have recently been fabricated by coupling carbon nanotubes to superconducting banks [7–10].

Now let us concentrate on the properties of the key element in the setup – AQD.

3. Energy and charge of AQD without Coulomb interaction.

The Andreev states give rise to new opportunities for tunable Josephson devices, e.g., the Josephson transistor [11, 12]; here, we are interested in their charge properties. We will consider the case of one transverse channel. In this case the problem effectively became one dimensional. We consider case of a large separation δ_{N} of resonances in the associated NININ problem (where superconductors S are replaced by normal metal N), $\delta_{\mathrm{N}} \gg \Delta$, such that a single Andreev level ε_{A} is trapped within the gap region. We are interested in sufficiently well isolated dot with a small width Γ_{N} of the associated NININ resonance, $\Gamma_{\mathrm{N}} \ll \Delta$. In this section, we completely neglect charging effects $E_{\mathrm{C}} = 0$. In summary, our device operates with energy scales $\Gamma_{\mathrm{N}} \ll \Delta \ll \delta_{\mathrm{N}}$.

The resonances in the NININ setup derive from the eigenvalue problem $\hat{\mathcal{H}}_0 \Psi = E\Psi$ with $\hat{\mathcal{H}}_0 = -\hbar^2 \partial_x^2 / 2m + U(x) - \varepsilon_{\mathrm{F}}$ and the potential $U(x) = U_{\mathrm{ps},1}(x + L/2) + U_{\mathrm{ps},2}(x - L/2)] + eV_{\mathrm{g}}\theta(L/2 - |x|)]$ describing two point-scatterers (with transmission and reflection amplitudes $T_l^{1/2} e^{\chi_l^t}$, $R_l^{1/2} e^{\chi_l^r}$; $R_l = 1 - T_l$, $l = 1, 2$) and the effect of the gate potential V_{g}, which we assume to be small as compared to the particle's energy E (measured from the band bottom in the leads), $eV_{\mathrm{g}} \ll E$. Resonances then appear at energies $E_n = \varepsilon_L(n\pi - \chi_1^r/2 - \chi_2^r/2)^2$; they are separated by $\delta_{\mathrm{N}} = (E_{n+1} - E_{n-1})/2 \approx 2E_n/n$ and are characterized by the width $\Gamma_{\mathrm{N}} = T\delta_{\mathrm{N}}/\pi\sqrt{R}$, where $\varepsilon_L = \hbar^2/2mL^2$. The bias V_{g} shifts the resonances by eV_{g}; we denote the position of the n-th resonance relative to ε_{F} by $\varepsilon_{\mathrm{N}} = E_n + eV_{\mathrm{g}} - \varepsilon_{\mathrm{F}}$.

We go from a normal- to an Andreev dot by replacing the normal leads with superconducting ones. In order to include Andreev scattering in the SINIS setup we have to solve the Bogoliubov-de Gennes equations (we choose states with $\varepsilon_{\mathrm{A}} \geqslant 0$)

$$\begin{bmatrix} \hat{\mathcal{H}}_0(x) & \hat{\Delta}(x) \\ \hat{\Delta}^*(x) & -\hat{\mathcal{H}}_0(x) \end{bmatrix} \begin{bmatrix} u \\ v \end{bmatrix} = \varepsilon_{\mathrm{A}} \begin{bmatrix} u \\ v \end{bmatrix}, \qquad (1)$$

with the pairing potential $\hat{\Delta}(x) = \Delta[\theta(-x - L/2)e^{-i\varphi/2} + \theta(x - L/2)e^{i\varphi/2}]$; $u(x)$ and $v(x)$ are the electron- and hole-like components of the wave function. The discrete states trapped below the gap derive from the quantization condition (in Andreev approximation)

$$(R_1 + R_2)\cos 2\pi \frac{\varepsilon_{\mathrm{A}}}{\delta_{\mathrm{N}}} - 4\sqrt{R_1 R_2}\sin^2 \alpha \cos 2\pi \frac{\varepsilon_{\mathrm{N}}}{\delta_{\mathrm{N}}} +$$

$$+ T_1 T_2 \cos\varphi = \cos\left(2\alpha - 2\pi \frac{\varepsilon_{\mathrm{A}}}{\delta_{\mathrm{N}}}\right) + R_1 R_2 \cos\left(2\alpha + 2\pi \frac{\varepsilon_{\mathrm{A}}}{\delta_{\mathrm{N}}}\right).$$

The phase $\alpha = \arccos(\varepsilon_{\mathrm{A}}/\Delta)$ is a phase acquiring at ideal NS boundary due to Andreev reflection with $\varphi = 0$. This formula can be directly obtained by using results of [12, 13].

We will consider the region $\Gamma_{\mathrm{N}}, |\varepsilon_{\mathrm{N}}| \ll \Delta$, so-called $\Delta \to \infty$ limit. With this strong inequality the quantization condition can be expanded and we obtain the following analytical expression

$$\varepsilon_{\mathrm{A}} = \sqrt{\varepsilon_{\mathrm{N}}^2 + \varepsilon_{\Gamma}^2}, \qquad (2)$$

where

$$\varepsilon_{\Gamma} = \frac{\Gamma_{\mathrm{N}}}{2}\sqrt{\cos^2 \frac{\varphi}{2} + A^2}, \quad A = \frac{|T_1 - T_2|}{2\sqrt{T_1 T_2}}. \qquad (3)$$

Andreev energy is phase sensitive when $|\varepsilon_{\mathrm{N}}| \lesssim \Gamma_{\mathrm{N}}$. In $\Delta \to \infty$ limit both $u(x)$ and $v(x)$ parts of wave function are nonzero only in the normal region

$$\begin{bmatrix} u(x) \\ v(x) \end{bmatrix} = \begin{cases} 0, & |x| > L/2, \\ \begin{bmatrix} C_{\mathrm{e}}^{\rightarrow} e^{ik_{\mathrm{e}}x} + C_{\mathrm{e}}^{\leftarrow} e^{-ik_{\mathrm{e}}x} \\ C_{\mathrm{h}}^{\leftarrow} e^{ik_{\mathrm{h}}x} + C_{\mathrm{h}}^{\rightarrow} e^{-ik_{\mathrm{h}}x} \end{bmatrix}, & |x| < L/2, \end{cases}$$

where $k_{\mathrm{e,h}} = [2m(\varepsilon_{\mathrm{F}} \pm \varepsilon_{\mathrm{A}})]^{1/2}/\hbar$ is the wave vectors of electrons and holes respectively. The coefficients are defined by $C_{\mathrm{e,h}}^{\rightarrow} = C_{\mathrm{e,h}}^{\leftarrow} = [(1 \pm \varepsilon_{\mathrm{N}}/\varepsilon_{\mathrm{A}})/2L]^{1/2}$.

The ground state of the system is the state $|0\rangle$ with energy $\varepsilon_0 \equiv U_0$ (counted from the Fermi energy ε_{F}) and without excited Bogolubov quasiparticles. The first excited state with one Bogolubov quasiparticle is doubly degenerated in spin $|1_\uparrow\rangle = \hat{a}_\uparrow^\dagger |0\rangle$, $|1_\downarrow\rangle = \hat{a}_\downarrow^\dagger |0\rangle$ and has energy $\varepsilon_1 = U_0 + \varepsilon_{\mathrm{A}}$. The doubly excited state with two quasiparticles $|2\rangle = \hat{a}_\uparrow^\dagger \hat{a}_\downarrow^\dagger |0\rangle$ has energy $\varepsilon_2 = U_0 + 2\varepsilon_{\mathrm{A}}$. The ground state energy can be expressed in terms of Andreev energy

$$U_0 = \varepsilon_{\mathrm{N}} - \varepsilon_{\mathrm{A}}. \qquad (4)$$

Here we omitted the term related to the contribution from the normal electrons below the Fermi surface which are not involved into the forming of the superconductivity; this term does not depend on φ.

The charge of the state $|\nu\rangle$ ($\nu = 0$, $1_\uparrow$, $1_\downarrow$, 2) can be obtained by differentiation of the corresponding energy ε_ν with respect to the gate voltage $q_\nu = \partial \varepsilon_\nu / \partial V_{\mathrm{g}}$ or by the averaging charge operator $\hat{Q} = e\sum_\sigma \int_{-L/2}^{L/2} \hat{\Psi}_\sigma^\dagger(x) \hat{\Psi}_\sigma(x)dx$ over the state

$|\nu\rangle$, $q_\nu = \langle\nu|\hat{Q}|\nu\rangle$. Here $\hat{\Psi}_\sigma(x) = \sum_n [u_n(x)\hat{a}_{n,\sigma} + \mathrm{sign}\sigma\, v_n^*(x)\hat{a}_{n,-\sigma}^\dagger]$; the sum is over all resonances. Both methods naturally give the same results

$$q_0 = e\left(1 - \frac{\varepsilon_N}{\varepsilon_A}\right), \quad q_1 = e, \quad q_2 = e\left(1 + \frac{\varepsilon_N}{\varepsilon_A}\right). \quad (5)$$

The only non-zero non-diagonal matrix element of the operator $\hat{Q}$ is q_{02}, $q_{02} = \langle 0|\hat{Q}|2\rangle = e(1 - \varepsilon_N^2/\varepsilon_A^2)^{1/2}$.

4. AQD with Coulomb interaction. In order to find the effect of week Coulomb interaction $E_C \ll \Delta$ at the limit Γ_N, $|\varepsilon_N| \ll \Delta$ we can disregard continuous states with the energies above the superconductive gap Δ and suppose that four levels of discrete spectrum form the whole basis of Hilbert space of the system. In four states basis we can make exact diagonalization of the Hamiltonian. The interaction is given by the operator

$$\hat{V} = E_C \frac{\hat{Q}^2}{e^2}.$$

The non-zero matrix elements of the operator $\hat{V}$ are

$$V_{00} = E_C(q_0^2 + q_{02}^2)/e^2, \quad V_{11} = E_C,$$
$$V_{22} = E_C(q_2^2 + q_{02}^2)/e^2, \quad V_{02} = 2E_C q_{02}/e.$$

The energy levels are defined by the compatibility condition of the following system

$$\begin{bmatrix} \tilde{\varepsilon}_0 - E & & & V_{02} \\ & \tilde{\varepsilon}_{1\uparrow} - E & & \\ & & \tilde{\varepsilon}_{1\downarrow} - E & \\ V_{20} & & & \tilde{\varepsilon}_2 - E \end{bmatrix} \begin{bmatrix} D_0 \\ D_{1\uparrow} \\ D_{1\downarrow} \\ D_2 \end{bmatrix} = 0,$$

where $\tilde{\varepsilon}_\nu = \varepsilon_\nu + V_{\nu\nu}$, $\nu = 0, 1_\uparrow, 1_\downarrow, 2$. The energy of the level with one Bogolubov quasiparticle $|1\rangle$ shifts to the constant

$$E_1 = \varepsilon_N + E_C, \quad (6)$$

does not mix with the other states, and degeneracy due to spin remains. This state is named Kramers doublet. The ground $|0\rangle$ and doubly excited $|2\rangle$ states mix due to Coulomb interaction and produce two new states, singlets $|-\rangle$ and $|+\rangle$; $|\pm\rangle = D_0^\pm |0\rangle + D_2^\pm |2\rangle$. The energies of these new states are

$$E_\pm = \varepsilon_N + 2E_C \pm \sqrt{(\varepsilon_N + 2E_C)^2 + \varepsilon_\Gamma^2}. \quad (7)$$

The energies of the doublet and singlet states depends on ε_N and φ in a different way and may cross; thus ground state can be formed by singlet $|-\rangle$ or by doublet $|1\rangle$; the state $|+\rangle$ always remains the second excited state, see Fig.2. When $E_C < \varepsilon_\Gamma$ the ground state
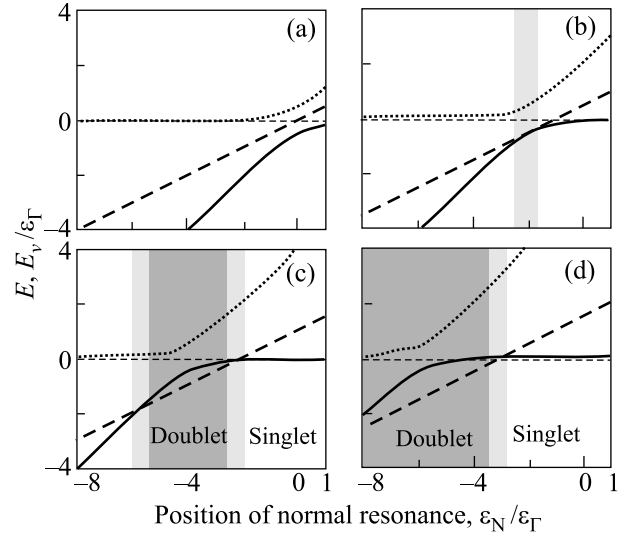

Fig.2. Energies E_- (solid line), E_1 (dashed line), and E_+ (dotted line) versus position of normal resonance. All energies are in units of ε_Γ (3). The Coulomb energy is $E_C = 0$ for (a), $E_C = \varepsilon_\Gamma$ for (b), $E_C = 2\varepsilon_\Gamma$ for (c), and $E_C = 3\varepsilon_\Gamma$ for (d). The doublet region appears when $E_C > \varepsilon_\Gamma$, see (b-d). In the filled region the ground state of the system is doublet; the width of this region is $2(E_C^2 - \varepsilon_\Gamma^2)^{1/2}$, edges of this region spreads due to finite temperature Θ

is singlet $|-\rangle$, elsewhere the ground state is doublet $|1\rangle$ in region

$$-2E_C - \sqrt{E_C^2 - \varepsilon_\Gamma^2} < \varepsilon_N < -2E_C + \sqrt{E_C^2 - \varepsilon_\Gamma^2} \quad (8)$$

and remains $|-\rangle$ at all the other values of ε_N [14]. At the edge of the region (8) singlet–doublet phase transition happens, with jump in the charge (see below).

The charges of the new states $|\mu\rangle$, $(\mu = 1, \pm)$ can be calculated as in previous section $Q_\mu = \partial E_\mu/\partial V_g$, it gives

$$Q_\pm = e\left(1 \pm \frac{\varepsilon_N + 2E_C}{\sqrt{(\varepsilon_N + 2E_C)^2 + \varepsilon_\Gamma^2}}\right), \quad Q_1 = e. \quad (9)$$

Everywhere except doublet region the ground state charge equals to Q_-, in doublet region the charge is pinned to the value $Q_1 = e$. As one can see from the Fig.3a,b for $E_C > E_C^* \equiv \Gamma_N A/2$ phase transition occur and the charge jumps to the value $\delta Q_{pt} = Q_- - Q_1$. At finite temperature this jump is smeared, see Fig.3c,d. The equilibrium charge with finite temperature Θ is

$$Q_{eq} = \frac{Q_- e^{-E_-/\Theta} + 2Q_1 e^{-E_1/\Theta} + Q_+ e^{-E_+/\Theta}}{e^{-E_-/\Theta} + 2e^{-E_1/\Theta} + e^{-E_+/\Theta}}, \quad (10)$$

here and below we set Boltzmann's constant $k_B = 1$.

5. Differential sensitivity. The differential sensitivity of equilibrium charge to the magnetic flux threading superconductive loop we defined as the absolute value
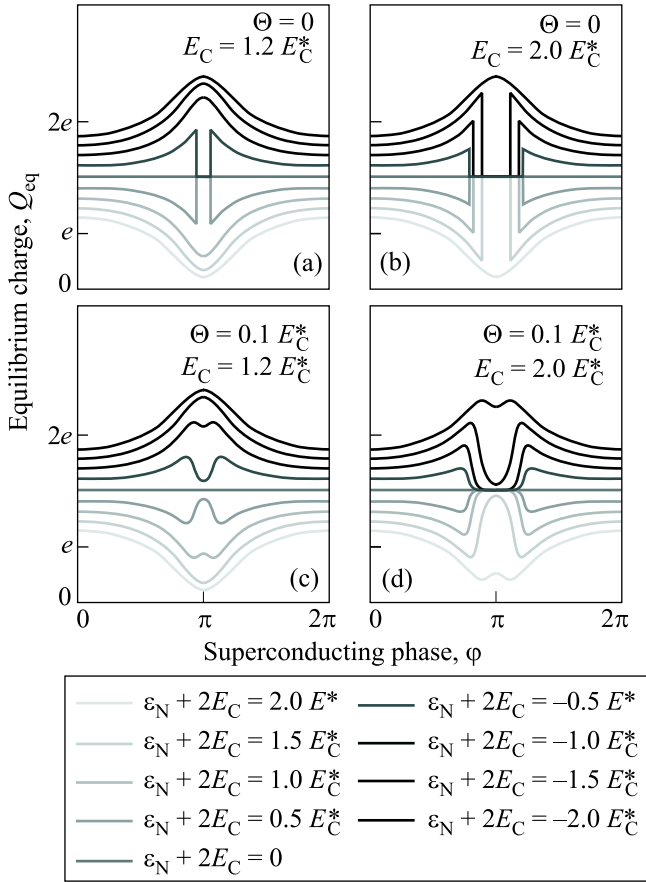
Fig.3. Equilibrium charge Q_{eq} (10) versus superconducting phase difference φ. At the figures (a) and (b) temperature is zero (i.e. Q_{eq} represents ground state charge), at (c) and (d) temperature is $\Theta = 0.1 E_C^*$, where $E_C^* \equiv \Gamma_N A/2$. The Coulomb energy is $E_C = 1.2 E_C^*$ for (a) and (c), $E_C = 2.0 E_C^*$ for (b) and (d). The asymmetry level of the dot is $A = 0.2$. The features at the centers of the plots corresponds to the doublet region (8). At (c) and (d) the border of doublet region is smoothed by temperature Θ. The curves differ by $\varepsilon_N + 2E_C$ values (from below, in units E_C^*): 2.0, 1.5, 1.0, 0.5, 0, -0.5, -1.0, -1.5, -2.0

of derivative $\partial Q_{eq}/\partial \Phi$ taken at the given value of magnetic flux[2], $S = |\partial Q_{eq}/\partial \Phi|$. By using (10) we obtain

$$S = \left| F_\Theta \frac{\partial Q}{\partial \Phi} + Q \frac{\partial F_\Theta}{\partial \Phi} \right|, \tag{11}$$

where $Q \equiv (Q_+ - Q_-)/2$, the derivative

$$\frac{\partial Q}{\partial \Phi} = e \frac{2\pi}{\Phi_0} \frac{(\varepsilon_N + 2E_C)\Gamma_N^2 \sin\varphi}{16\left[(\varepsilon_N + 2E_C)^2 + \varepsilon_r^2\right]^{3/2}} \tag{12}$$

---

[2] Note that the sensitivity of charge-to-flux convertor $S \equiv$ $\equiv S_{\Phi \to Q}$ coincides with the voltage-to-current sensitivity of Josephson transistor that is described in [12] $S_{V \to J} = |\partial J/\partial V_g|$.

and function

$$F_\Theta = \frac{e^{-E_+/\Theta} - e^{-E_-/\Theta}}{e^{-E_-/\Theta} + 2e^{-E_1/\Theta} + e^{-E_+/\Theta}}. \tag{13}$$

As one can see form the Fig.3 there are two intervals, where $Q_{eq}(\varphi)$ dependence is steep. As φ increases from $\varphi = 0$ the charge increases (decreases) and reaches maximum (minimum). Until $E_C < E_C^*$ the maximum (minimum) of charge is always at $\varphi = \pi$. At $E_C > E_C^*$ the extremum splits and in between two extremums second interval with steep dependence emerges. The first interval (interval I in what follows) corresponds to the singlet state of the AQD, the second (interval II in what follows) to the doublet state. We start with describing of the first interval. We fix parameters Γ_N, A, and E_C and search for the maximum of sensitivity S as a function of ε_N and φ. The non-trivial symmetries $Q_{eq}(\varphi, \varepsilon_N) = Q_{eq}(2\pi - \varphi, \varepsilon_N)$, $Q_{eq}(\varphi, \varepsilon_N) - Q_{eq}(\varphi, 0) =$ $= -Q_{eq}(\varphi, -\varepsilon_N - 4E_C) + Q_{eq}(\varphi, 0)$ allow us to restrict search region to $0 \leqslant \varphi \leqslant \pi$, $\varepsilon_N + 2E_C \geqslant 0$. Then we analyze the maximum of S as a function of E_C keeping A and Γ_N constants.

Interval I. In the case $E_C \leqslant [3(1+A^2)/(1+2A^2)]^{1/2} E_C^*$ and zero temperature $\Theta = 0$ the function $F_\Theta = 1$ and the sensitivity is totally defined by the derivative $\partial Q/\partial \Phi$ (12). The function $|\partial Q/\partial \Phi|$ has a maximum at $\varepsilon_N + 2E_C = E_C^*[(1 + A^2)/(1 + 2A^2)]^{1/2}$ and $\varphi = \pi - 2\arcsin[A/(1 + 2A^2)^{1/2}]$, it equals

$$S_{max}^I = |e| \frac{2\pi}{\Phi_0} \frac{1}{6\sqrt{3}A\sqrt{1 + A^2}}. \tag{14}$$

One can see that the smaller A the bigger sensitivity. In other words more symmetric SINIS structure provides better sensitivity. When $\Theta \ll E_C^*$ the sensitivity is nearly independent on temperature.

In the opposite case $E_C \geqslant [3(1+A^2)/(1+2A^2)]^{1/2} E_C^*$ the doublet region absorbs maximum (14) and maximal value of sensitivity is always at the outer edge of the region (8). It gives maximum

$$S_{max}^I = |e| \frac{2\pi}{\Phi_0} \frac{\Gamma_N^3}{48\sqrt{3}E_C^3} \times$$
$$\times \sqrt{2(\lambda^2 - \lambda + 1)^{3/2} - (\lambda + 1)(\lambda - 2)(2\lambda - 1)} \tag{15}$$

at $\varepsilon_N + 2E_C = (\Gamma_N/2)\{[2\lambda - 1 + (\lambda^2 - \lambda + 1)^{1/2}]/3\}^{1/2}$ and $\varphi = 2\arccos\{[\lambda + 1 - (\lambda^2 - \lambda + 1)^{1/2}]/3\}^{1/2}$, where $\lambda = (E_C^2 - E_C^{*2})/(\Gamma_N/2)^2$. In the limit $E_C \gg \Gamma_N$, E_C^* formula (15) reduces to

$$S_{max}^I \approx |e| \frac{2\pi}{\Phi_0} \frac{\Gamma_N^2}{16E_C^2} \tag{16}$$

and maximum reaches at $\varepsilon_{\mathrm{N}} + 2E_{\mathrm{C}} \approx E_{\mathrm{C}} - \Gamma_{\mathrm{N}}^2/16E_{\mathrm{C}}$ and $\varphi \approx \pi/2 + \Gamma_{\mathrm{N}}^2/16E_{\mathrm{C}}^2$.

Interval II. At zero temperature there is a jump in the charge at the edges of interval II, and thus the sensitivity diverges at this points. Finite temperature smears the jump and the sensitivity becomes finite. In the case $E_{\mathrm{C}} \gg \Theta$, Γ_{N}, E_{C}^* the maximum of the sensitivity again located near point $\varepsilon_{\mathrm{N}} + 2E_{\mathrm{C}} = E_{\mathrm{C}}$, $\varphi = \pi/2$ and can be estimated as

$$S_{\max}^{\mathrm{II}} \approx |e| \frac{2\pi}{\Phi_0} \frac{\Gamma_{\mathrm{N}}^2}{64 E_{\mathrm{C}} \Theta}. \quad (17)$$

At arbitrary E_{C} the expression for $S_{\max}^{\mathrm{II}}$ is not solvable by quadratures. We plot the dependence $S_{\max}^{\mathrm{II}}(E_{\mathrm{C}})$ numerically at Fig.4. At the same plot we present also
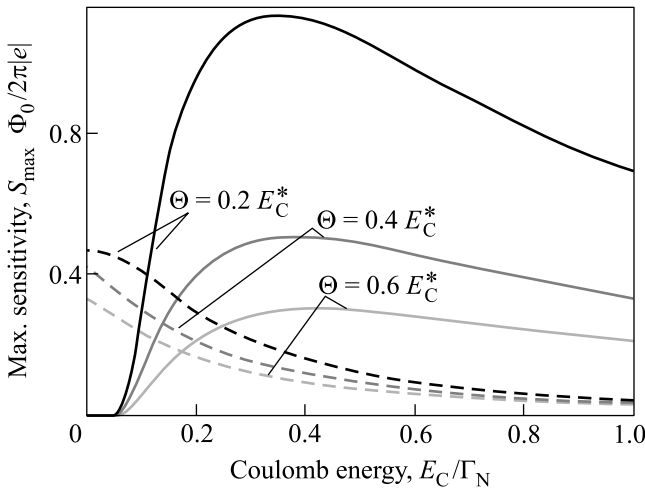

Fig.4. Maximum of the differential sensitivity in the interval I $S_{\max}^{\mathrm{I}}$ (dashed lines) and in the interval II $S_{\max}^{\mathrm{II}}$ (solid lines) versus Coulomb energy E_{C}. The asymmetry level is $A = 0.2$, correspondent critical Coulomb energy is $E_{\mathrm{C}}^*/\Gamma_{\mathrm{N}} = 0.1$. The temperature varies from $\Theta = 0.2E_{\mathrm{C}}^*$ up to $\Theta = 0.6E_{\mathrm{C}}^*$, see insert in the plot

the maximum of the sensitivity from the interval I. One can see that at big Coulomb interaction the region of the smeared phase transition always provides sharper $Q_{\mathrm{eq}}(\varphi)$ dependence.

In realistic nanodevices Coulomb energy can be smaller than Γ_{N} (see discussion in [7, 2]), but one also can make it bigger than Γ_{N}, e.g. increasing Fermi energy in the quasi-one dimensional normal region.

6. Conclusion. In this article we pointed out that the φ-dependence of AQD charge in principal may be used for new type of magnetometers which works according to the scheme "magnetic flux–AQD charge–

SET–current" instead of usual SQUIDs scheme "magnetic flux–current". We analyzed charge sensitivity as a function of magnetic flux, gate voltage, Coulomb interaction, asymmetry of the dot, and temperature.

The sensitivity of our setup can be further increased by adding electromechanical element [15]. If one apply big electric field to the charged nanowire, the change in the charge will lead to the mechanical shift of the wire. This shift can be then detected due to the change of the capacitance of the whole setup as in [15].

We concentrated here on strictly 1-channel wire to demonstrate the effect. The case of n-channel wire ($n = 2$ or $n > 2$) can be analyzed in the same technique and we plan consider it nearest time.

1. B. D. Josephson, Rev. Mod. Phys. **46**, 251 (1974).

2. I. A. Sadovskyy, G. B. Lesovik, and G. Blatter, Phys. Rev. B **75**, 195334 (2007).

3. K. Engström and J. Kinaret, Phys. Scr. **70**, 326 (2004).

4. R. Kleiner, D. Koelle, F. Ludwig, and J. Clarke, Proceed. of the IEEE **92**, 1534 (2004).

5. J. Clarke and A. I. Braginski, Ed. *SQUID Handbook*, Berlin, Germany: WileyЦVCH, 2004.

6. A. Aassime, G. Johansson, G. Wendin et al., Phys. Rev. Lett. **86**, 3376 (2001).

7. P. Jarillo-Herrero, J. A. van Dam, and L. P. Kouwenhoven, Nature **439**, 953 (2006).

8. J. A. van Dam, Yu. V. Nazarov, E. P. A. M. Bakkers et al., Nature **442**, 667 (2006).

9. J.-P. Cleuziou, W. Wernsdorfer, V. Bouchiat et al., Nature nanotechnology **1**, 53 (2006).

10. M. R. Buitelaar, T. Nussbaumer, and C. Schönenberger, Phys. Rev. Lett. **89**, 256801 (2002).

11. H. van Houton, Appl. Phys. Lett. **58**, 1326 (1991); G. Wendin and V. S. Shumeiko, Superlattices and Microstructures **20**, 569 (1996).

12. D. D. Kuhn, N. M. Chtchelkatchev, G. B. Lesovik, and G. Blatter, Phys. Rev. B **63**, 054520 (2001).

13. N. M. Chtchelkatchev, G. B. Lesovik, and G. Blatter, Phys. Rev. B **62**, 3559 (2000).

14. A. V. Rozhkov and D. P. Arovas, Phys. Rev. B **62**, 6687 (2000).

15. R. G. Knobel and A. N. Cleland, Nature **424**, 291 (2003).